Anionic synthesis and end-functionalization of polymyrcene in a flow microreactor system

Katia Pérez, Sébastien Leveneur, Fabrice Burel, Julien Legros, Daniela Vuluga

Anionic synthesis and end-functionalization of polymyrcene in a flow microreactor system

fReceived 00th January 20xx,
Accepted 00th January 20xx

DOI: 10.1039/x0xx00000x

Katia Pérez,[a,b] Sébastien Leveneur,[c] Fabrice Burel,[a] Julien Legros,[b] and Daniela Vuluga*[,a]

In the search for flexible and sustainable methods for the synthesis of macromolecular scaffolds, microflow systems exhibit unrivalled qualities, as exemplified by the fine control on mass and thermal transfers. Therefore, the development of the polymerization of a bio-based monomer under flow conditions represents a major topic in the current context. In order to provide a system combining safer conditions and a firm grip on polymerization, we now report that the anionic polymerization of myrcene can be finely tuned in a microflow reactor to afford low molar mass polymyrcene (PMYR). We also showed that carbon dioxide could be trapped, with a further inlet onto the telescoped flow set-up, to introduce a carboxylic acid ending onto PMYR. In parallel, a kinetic model that can perfectly predict the outcome of the polymerization under such flow conditions has been developed.

Introduction

In the framework of sustainable development over the last decade, the interest of scientists towards bio-sourced materials has become obvious, and terpene derivatives have thus been widely studied to obtain different types of materials.[1–5] Due to the presence of several double bonds in their structure, terpenes can easily be considered as monomer substitutes for polybutadiene, a prominent member of the commodity polymers. Among the most interesting monomers of this family, myrcene (owing a isoprene motif) has been polymerized by various pathways, radical,[6,7] anionic,[8] or coordinative,[9] leading to polymyrcene (PMYR) high molar mass (*Mn* 20000-60000) with low dispersity (1.3<*Đ*<2.0).[9–11] However, the preparation of materials with interesting architectures and properties is highly depending on the controlled size of the polymers (*ie* oligomeric) that will be embedded. In addition, it is necessary to introduce functional groups on these oligomers to transform them into reactive entities able to be integrated into the materials. Thus, the quest for a flexible and sustainable method for the controlled polymerization of myrcene into oligomers is a tackling challenge.

However, the sustainability of a chemical reaction/process must be considered as a whole; if most of the concerns focus on the substrate source and the reagents/solvents involved the tools used to perform this transformation and the energy consumed are as important as the other parameters. In this sense, miniaturised reactors working in continuous flow have been shown to be invaluable tools to perform reactions with excellent grip on mass and heat transfer, allowing thus to reach high selectivity without cryogenic conditions, sometimes unavailable under classical batch conditions.[12–14] Moreover, such devices offer the possibility to handle and treat large volumes of chemicals -even hazardous- without exposing the operator.[15–20] Thus, the handling of pyrophoric alkyl lithiums can be easily done in a flow system and very selective and challenging transformations have been reported with incomparable results with regard to conventional batch conditions.[21–29] Such organolithium compounds are very useful promoters of anionic polymerization and flow polymerization of reactive petroleum-based olefins (acrylate, styrenes) has been successfully reported by Yoshida and Nagaki.[30–35] Along these lines, we now report that the polymerization of myrcene (a biobased analogue of isoprene) can be finely controlled to afford low molar mass PMYR, with the kinetics supported by a predictive model. As a proof of concept for the functionalization of PMYR in an integrated flow device, we also demonstrate that a carboxylic acid moiety can be easily introduced from CO_2 (Figure 1).

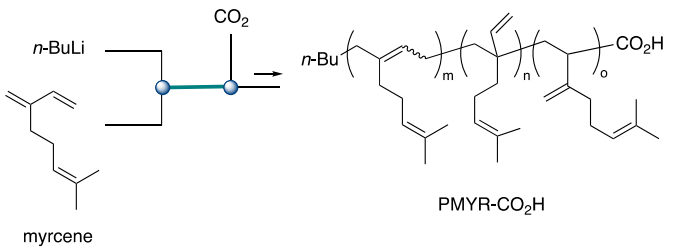

Fig. 1. Microflow synthesis of PMYR by anionic polymerization

[a.] *INSA Rouen, Normandie Univ, UNIROUEN, CNRS, PBS, 76000 Rouen, France*
e-mail : daniela.vuluga@insa-rouen.fr
[b.] *CNRS, INSA Rouen, Normandie Univ, UNIROUEN, COBRA, 76000 Rouen, France.*
[c.] *INSA Rouen, Normandie Univ, UNIROUEN, LSPC, UR4704, 76000 Rouen, France.*
† Electronic Supplementary Information (ESI) available: Experimanetal setups and analytical data. See DOI: 10.1039/x0xx00000x

Experimental section

General information

Chemicals. Myrcene was purchased from Sigma-Aldrich or Acros (distilled from CaH_2) and dissolved in anhydrous THF (distilled from benzophenone/sodium) for the reaction. *n*-Butyl lithium was purchased from Sigma-Aldrich or Acros as a 2.5 M solution in hexanes and diluted to the desired title with *n*-hexane (distilled from CaH_2), and titrated by menthol/bipyridine method before usage. Methanol was purchased from Sigma-Aldrich or Acros and was used as provided. TMSCl was freshly distilled. Carbon dioxide (CO_2 purity > 99.995 vol%, H_2O<5 ppm) was purchased from Linde (CO_2 4.5).

Materials. Stainless steel tubing, adapters, ferrules and connections were purchased from CIL-Cluzeau. Micromixers were custom manufactured by MG-63 (vide infra for schematics). Reagents were fed in the reactors with Harvard Apparatus PHD Ultra syringe pumps, and SGE gas-tight glass syringes.

Analytical methods. NMR analysis: The ^{1}H and ^{13}C NMR Spectra were recorded on a Bruker 300 MHz spectrometer and worked with MestReNova software, chemical shifts are given in part per millions (ppm) relative to de residual solvent (7.26 and 77.16 respectively for $CDCl_3$). Spectra were calibrated on residual non-deuterated solvent peaks.

Gel Permeation Chromatography (GPC): GPC chromatograms were recorded on a PL-GPC 50 Plus, treated with GPC offline software. GPC was calibrated with polymethyl methacrylate (PMMA) a pre-weighed polymer standard from Agilent. Samples were diluted in dichloromethane and injected into the GPC (30 °C, 1 mL/min, 2 mixed-C column).

Infrared analysis: infrared spectra were recorded on a Perkin Elmer ATR universal sampler 100 spectrum.

Typical procedures

Anionic polymerization under batch conditions. All experiments were run in oxygen- and moisture-free environment. Glassware was dried under vacuum using a Schlenk line by heating the flask with a heat-gun before cycling dry argon and vacuum. 2.6 mL of anhydrous THF is introduced in a 50 mL-round bottom flask under inert atmosphere (Ar) and then cooled with a 10 °C water bath. Then, 1.4 mL of hexane is introduced and 0.19 mL of *n*-BuLi (2.5 M in hexanes) is introduced under stirring. After 5 minutes, 1.4 mL of myrcene (8 mmol) is introduced in one portion. After the time selected (1, 2, 8 min, etc.), the reaction is quenched with a methanol/water mixture (2:2 mL). The resulting solution is then extracted with dichloromethane (3×10 mL), washed with water (20 mL), dried over magnesium sulfate, and concentrated under vacuum to afford a crude mixture, analyzed by mean of NMR.

Anionic polymerization under flow conditions. Stainless steel reactors were dried overnight in an oven at 120 °C, before cooling in a dessicator over silica gel under vacuum. The flow system is composed of a first inlet containing a solution of myrcene in THF (2 M) and a second inlet with *n*-BuLi solution (0.3 M in hexanes). The solutions are passed through a first T-shaped micromixer (stainless steel, 500 µm of internal diameter (ID)) connected to a tubular microreactor (stainless steel, 750 µm ID, 1 m length) at the desired flow rate. This microreactor is immersed in a water bath thermostated at 10° C. The reaction mixture then feed a second T-shaped micromixer (500 µm ID) to be quenched with methanol (flow rate 0.1 mL/min). The quenched mixture is passed through a second tube of 300 mm length and 750 µm ID before collection in a vial containing 2 mL of HCl 2 N (three dead volumes of reagents were run through the system before collection to ensure reactor equilibrium, approximately between 2 and 5 mL were collected for analysis). The quenched mixture is extracted with dichloromethane (3 x 10 mL), washed with water (20 mL), dried over magnesium sulfate, and concentrated under vacuum to afford a crude mixture, analyzed by NMR.

Polymerization and functionalization with TMS under flow conditions. The flow system is composed of a first inlet containing a solution of myrcene in THF (2 M) and a second inlet with *n*-BuLi solution (0.3 M in hexanes). The solutions are passed through a T-shaped micromixer (stainless steel, 500 µm of internal diameter (ID)) connected to a microreactor (stainless steel, 750 µm ID, 3 m length) at the desired flow rate. This microreactor is immersed in a water bath thermostated at 10 °C. The resulting solution is introduced in a second T-shaped micromixer (500 µm ID) connected to a trimethylsilyl chloride (TMSCl) inlet. The mixture is passed through a second tube of 300 cm length and 750 µm ID before collection in a vial containing 2 mL of HCl 2 N. The procedure for collection, extraction and analysis of the sample was performed as above.

Telescoped polymerization and functionalization with CO_2 under flow conditions. For the functionalization of polymyrcene with CO_2 a similar system in continuous flow was used as previously mentioned above. However, in the second micromixer, instead of methanol, CO_2 gas is introduced by connecting a gas tank to a mass flow controller (Bronkhorst High-Tech BV). This inlet is connected to a second reactor (Reactor 2: ID = 0.75 mm, L = 30 cm) to generate the PMYR functionalized with a carboxyl group, before collection in a vial containing 2 mL of HCl 2 N. The procedure for collection, extraction and analysis of the sample was performed as above.

Results and discussion

This section describes the anionic polymerization of myrcene under batch and flow conditions, in order to get polymyrcene (PMYR) with finely controlled molar mass, and also to introduce a carboxylic acid moiety on PMYR by direct carbon dioxide incorporation.

Polymerization under batch conditions

First experiments were performed under batch conditions in a simple flask under stirring in a thermostated bath at 10 °C as already performed for anionic polymerization.[36] Whereas *s*-BuLi is mostly used for this purpose, *n*-BuLi is also efficient but the latter is much more stable in ethereal solvents in a broader range of temperatures, preventing the competitive

decomposition of THF via reverse (3+2) cycloaddition when non-cryogenic conditions are applied.[37,38] The results of the polymerization of myrcene into PMYR with *n*-BuLi (myrcene/*n*-BuLi = 17:1, providing a theoretical mass of 2316 g/mol) at various scales (from 110 mg to 17 g) at various reaction times are provided in Table 1.

Table 1. Anionic polymerization of myrcene with *n*-BuLi in batch at various scales.[a]

Entry	Quantity of myrcene (g)	*t* (min)	*Mn* ^{1}H RMN (g/mol)[b,c]	*Mn* GPC (g/mol) [b]	*Đ*	Yield (%)[d]	Conv. (%)[e]	*Mn* theo.[f]
1	0.110	2	650	600	1.23	28	28	648
2		10	1050	1300	1.26	53	45	1227
3		20	2200	1850	1.19	71	95	1644
4		30	2400	1900	1.23	91	104	2107
5	1	1	970	900	1.24	20	42	463
6		2	800	950	1.14	32	35	741
7		4	1700	1600	1.12	61	73	1412
8		8	2330	2050	1.14	90	101	2084
9		10	2200	2800	1.24	59	95	1366
10		30	2700	3250	1.23	68	117	1574
11		60	2600	3000	1.35	65	112	1505
12	17	1	2060	2300	1.13	88	89	2038
13		10	2100	2000	1.17	92	91	2130

[a] Performed at 10 °C with myrcene/*n*-BuLi = 17:1. [b] Average molecular weight. [c] ^{1}H NMR yields are calculated by comparison of the relative intensity of CH_3 group of the initiator (δ = 0.87 ppm) with that of vinyl CH of PMYR (δ = 4.75 ppm). [d] based on the mass of PMYR recovered after full removal of volatiles (including myrcene). [e] based on the Mn (^{1}H NMR)/2316×100. [f] Theoretical Mn = yield×2316/100.

Adding 110 mg of myrcene to a *n*-BuLi /THF solution, allowed to obtain increasing masses of polymer according to reaction time (entries 1-4). Thus, quenching with methanol after 2 min yielded an oligomer with 4 units (M = 650). Increasing the reaction time allowed to gain mass up to 2400 after 30 min, with intermediate values M = 1050 (10 min), 2200 (20 min). It is therefore possible to finely control the polymerization process to reach precise molar mass (Mn) value for tailored made oligomers with a small amount of starting materials. Increasing the amount of myrcene to 1 g afforded M = 970 after only 1 min (entry 5) and a maximum molar mass M= 2330 was obtained after 8 min (entry 8). A significant scale up was finally performed on 17 g of myrcene. In this case, the effect of the scale was tremendous since a single minute reaction allowed to reach M = 2060 (entry 12). Such an effect of the quantity of starting materials on the reaction rate can only be attributed to an (expected) exothermic behavior of the reaction despite the bath thermostated at 10 °C. Thus, the reaction was reproduced in the presence of a thermal probe inside the reaction medium: as soon as the myrcene was added to the medium the reaction jumped from 10 to 50 °C within 2 minutes. Regarding dispersity (*Đ*), the values obtained are regular and in the classical range for anionic polymerization (<1.5).

From the experiments reported in Table 1, the following conclusions can be drawn: it is possible to generate custom made oligomers from an anionic process with a precise number of units provided that the reaction is performed on a very small scale (*ca*. 100 mg). As soon as the scale is increased, an uncontrolled exothermic process occurs leading to a competitive consumption of organolithium species (*vide supra*),[37,38] with an increase in the monomer/organolithium ratio, provoking thus a rapid and uncontrolled gain in molar mass. Therefore, the obtaining of small oligomers in high amounts cannot be obtained under batch conditions.

It must be noted that, for the 17 g experiment, lower final molar masses are observed probably because *n*-BuLi is used directly from the commercial bottle, as provided (conversely to the experiments performed on lower scales (0.11 and 1.0 g) where it was dissolved prior to use), avoiding thus early degradation of the initiator.

Polymerization under microflow conditions

Flow microreactors exhibit unique features that perfectly fit with our purpose: the size of the reactor allows to react extremely small quantity of monomers within a subminute reaction time,[30–33,35] with expected highly positive consequences on the precise control of the molar mass of the PMYR. Moreover, the thermal transfers are extremely well mastered as well avoiding the process to get out of hand. It is also worth noting that since the reactor is working under continuous flow, the quantity of PMYR produced is related to the operating time of the reactor rather than on the size of the reactor (ie under batch conditions). Thus, we implemented a flow set-up for the anionic polymerization of myrcene, as depicted in Figure 2.

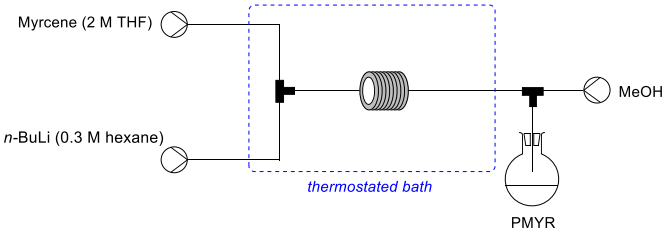

Fig. 2. Flow polymerization of myrcene.

Our experiments were thus performed with a flow system equipped with a stainless steel reactor composed of a T-shaped mixer and tubing with ID = 750 µm, the outlet being collected in an aqueous acidic solution (Table 2).

Table 2. Anionic polymerization of myrcene with *n*-BuLi under flow conditions at various temperatures and scales.[a,b]

Entry	*T* (°C)	*Mn*[c,d] ^{1}H RMN (g/mol)	*Mn*[c] GPC (g/mol)	*Đ*	Yield (%)[e]	Conv. (%)[f]	*Mn* theo.[g]
1	10	700	650	1.27	28	30	648
2	20	1100	1000	1.23	43	47	996
3	30	1350	1050	1.18	65	58	1505
4	40	1500	1200	1.19	73	65	1690
5	50	1350	1200	1.21	58	58	1343

[a] According to set-up depicted in Fig. 2. [b] Myrcene/n-BuLi flow rate (mL/min) : 0.25/0.1 (68 mg/min for myrcene); t^R = 75 s; L(reactor) =1 m; ID(reactor) = 0.7 mm; [myrcene] in THF = 2 M; [n-BuLi] in hexane = 0.3 M. [c] Average molecular weight. [d] Calculated by comparison of the relative intensity of CH_3 group of the initiator (δ = 0.87 ppm) with that of vinyl CH of PMYR (δ = 4.75 ppm). [e] based on the mass of PMYR recovered after full removal of volatiles (including myrcene). [f] based on the Mn (^{1}H NMR)/2316×100. [g] Theoretical Mn = yield×2316/100.

The first experiments (entries 1-5, table 2) were performed to determine the influence of the temperature at constant t^R = 75 s. At this fast reaction time, a temperature of 10 °C allowed to reach a short Mn = 700 (ie 5 monomer units) whereas 20 °C led to Mn = 1100 (8 units) with a plateau at 30 °C with Mn = 1350 (10 units). Therefore, performing the reaction at a temperature close to room temperature (10 to 20 °C) is energy saving and allows fine control of the Mn of PMYR. Moreover it avoids the competitive decomposition of THF in presence of organolithium bases at higher temperatures.[37–39]

Regarding the microstructure of PMYR obtained by anionic polymerization, the effect of the solvent has been highlighted in two distinct papers: Avila-Ortega reported that the reaction of myrcene in pure benzene with *s*-BuLi afforded 1,4 microstructure as major isomer (85%) while Hillmeyer and Hoye described the 3,4 isomer as major product (60%) along with 1,4 (30%) and 1,2 (10%) adducts in THF with *s*-BuLi (1.4 M in hexanes).[40,41] An NMR comparison of the structures obtained herein under batch and flow conditions were also performed. In batch, it showed that the 3,4 isomer is the major adduct (57%) along with 1,4 (33%) and 1,2 isomers (10%). In flow, the proportion of the 3,4 isomer rises to 66% accompanied with 1,4 (22%) and 1,2 (12%). However, this is hardly assignable to the nature of the reactor, but rather to the proportion of hexanes in the polymerization medium. Whereas, in batch, *n*-BuLi was used as provided (2.5 M in hexanes), the commercial solution was diluted to 0.3 M for practical reasons in the flow inlet. This results in a significant variation of the V/V percentage of hexanes in the reaction medium (hexanes/THF): 14% (batch) and 29% (flow) with obvious consequences on the reactivity and selectivity.[42]

The influence of the residence time t^R was further evaluated at both these temperatures from t^R = 19 to 600 s by modifying the flow rates in a fixed length reactor (L = 0.5 m; entries 1-6, table 3). As expected, the molar mass increased according to t^R as well as to the temperature. For example, the increase goes from Mn = 400 to 800 at 10 °C, and from 450 to 1100 at 20 °C. By working at a precise residence time, either by varying the flow rate or the reactor length, gave the same results. This means that mixing (influenced by the flow rate in the mixing zone) does not seem to be a major parameter in this reaction between *n*-BuLi (in hexane) and myrcene (in THF). Probably because an instantaneous anionic initiation of myrcene by *n*-BuLi occurs even at low flow rates in our conditions (THF). Thus, the t^R can be tuned either through the flow rate or the reactor size, indifferently. This was also confirmed by results reported in entries 9-11. Therefore, we chose to perform final experiments for the controlled synthesis of low-Mn PMYR at fixed flow rate with various reactors at 10°C (entries 12-19) and 20 °C (entries 20-25). With the flow system it is therefore possible to precisely select the number of monomer units with Mn = 450 (t^R = 19 s; entry 4) to 2100 (t^R = 600 s; entry 19). It is worth to note that such a fine t^R tuning (and therefore Mn of PMYR) is unreachable in a conventional batch reactor.

In order to confirm the living character of the polymerization, it was decided to trap a relevant group instead of a simple hydrogen atom. Indeed, whereas this hydrogen should come from the methanol inlet, competitive processes could also occur (such as deprotonation of THF) and quench the polymerization in an early manner. For this, an inlet of TMSCl was connected to the flow polymerization reactor (Fig. 3).

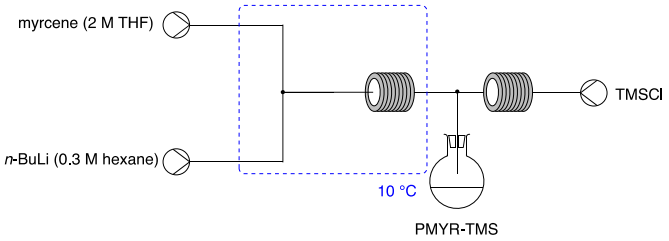

Fig. 3. Assessment of living polymerization in the flow microreactor.

A representative experiment was performed with t^{R2} = 227 s, and the degree of functionalization was determined by ^{1}H NMR analyses by comparing the $(CH_3)_3$ groups from TMS with the CH_3 group from the *n*-Bu initiator: a 73% degree of functionalization was measured, showing thus the living character of this process. It should be noted that the uncomplete functionalization of the polymer with the TMS group is much likely due to the traces of HCl in the TMSCl (injected neat).

From these results it can be concluded that, in a flow system, an anionic living polymerization of myrcene can be performed in a flow microreactor: the molar mass (Mn) of PMYR can be modulated by adapting the residence time and the temperature within the flow reactor, conversely to batch polymerization which depends on the amount of material used. Thus, a kinetic model can be of interest to better apprehend this type of reaction under flow conditions.

Table 3. Anionic polymerization of myrcene with *n*-BuLi under flow conditions, different scales at 10 °C and 20 °C.[a]

Entry	*T* (°C)	t^R (s)	L (m)[b]	*Mn* ^{1}H RMN (g/mol) [c,d]	*Mn* GPC (g/mol) [c]	*Đ*	Yield (%)[e]	Conv (%)[f]	*Mn* theo.[g]
1	10	19	0.5	400	300	1.18	10	17	231
2		38		450	400	1.44	13	19	301
3		75		800	650	1.10	26	35	602
4	20	19	0.5	450	400	1.25	18	19	416
5		38		700	600	1.25	26	30	602
6		75		1100	900	1.30	40	47	926
7	10	38	8.0	600	350	1.16	29	26	671
8		75		900	550	1.23	47	39	1088
9	10	75	0.5	800	650	1.10	26	35	602
10			1.0	700	650	1.27	28	32	648
11			8.0	850	550	1.23	47	37	1088
12	10	38	0.5	450	400	1.44	13	19	301
13		75	1.0	700	600	1.27	28	30	648
14		120	1.6	1000	850	1.33	42	43	972
15		157	2.0	1150	900	1.19	54	50	1250
16		180	2.4	1300	1050	1.16	57	56	1320
17		227	3.0	1050	1200	1.43	47	45	1088
18		302	4.0	1500	1400	1.20	69	65	1598
19		600	8.0	2100	1700	1.36	54	91	1250
20	20	38	0.5	900	600	1.25	40	39	926
21		75	1.0	1100	850	1.26	51	47	1181
22		120	1.6	1450	1050	1.36	78	63	1806
23		157	2.0	1650	1450	1.36	73	71	1690
24		180	2.4	1500	1500	1.34	78	65	1806
25		302	4.0	1700	1800	1.18	74	73	1713

[a] ID(reactor) = 0.7 mm; [myrcene] in THF = 2 M; [n-BuLi] in hexane = 0.3 M; flow rates are adjusted according to $t^R = V_{reactor}/Q$. [b] Reactor length. [c] Average molecular weight. [d] Calculated by comparison of the relative intensity of CH_3 group of the initiator (δ = 0.87 ppm) with that of vinyl CH of PMYR (δ = 4.75 ppm). [e] based on the mass of PMYR recovered after full removal of volatiles (including myrcene). [f] based on the Mn (^{1}H NMR)/2316×100. [g] Theoretical Mn = yield×2316/100.

Kinetic modeling of myrcene polymerization in continuous flow

Non-ideal mixing conditions could occur in batch conditions, decreasing the accuracy of kinetic constant evaluation. To overcome such issue, microfluidic conditions was used to estimate kinetic constants for myrcene polymerization.

The study of anionic myrcene polymerization in batch conditions was performed by Gonzalez-Villa et al. in 2019. This study was carried out in cyclohexane initiated by *n*-butyllithium at different temperatures (55, 63, and 71 °C). For example, at 55 ° C a propagation constant of kp = 1.24 L(1/b)/ (mol^ (1/b)*min) was evaluated.[43] The anionic polymerization myrcene follow the reaction path depicted in Figure 4.

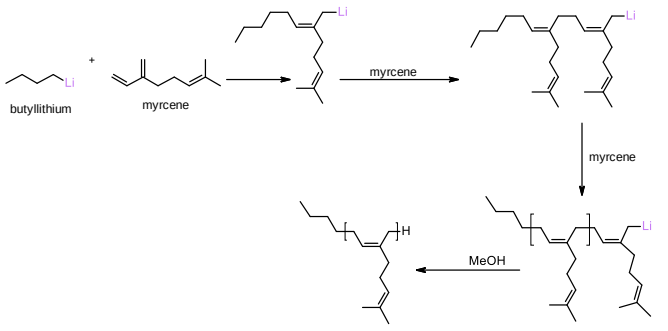

Fig. 4. Reaction path for the anionic polymerization of myrcene.

The reaction rates of step 1 and 2 were expressed as:

$$R_1 = k_1[nBuLi][myrcene]$$
$$R_2 = k_2[Intermediate][myrcene]$$

We assumed a plug flow model for the continuous reactor. The material balances are expressed as:

$$\frac{\partial C_i}{\partial \tau} = r_i \qquad \text{Equation 1}$$

Thus, the material balance for each compound is:

$$\frac{\partial [M]}{\partial \tau} = -R_1 - R_2 \qquad \text{Equation 2}$$

$$\frac{\partial [Int]}{\partial \tau} = R_1 - R_2 \qquad \text{Equation 3}$$

$$\frac{\partial [Dim]}{\partial \tau} = +R_2 \qquad \text{Equation 4}$$

$$\frac{\partial [BuLi]}{\partial \tau} = -R_1 \qquad \text{Equation 5}$$

The kinetic modeling was performed in ModEst software; ODEs were solved by ODESSA solver.[44,45]

Myrcene concentration was used as an observable. The objective function was defined as OF= $([M]_{exp}-[M]_{sim})^2$.

The minimization of the objective function was done by the simplex and Levenberg-Marquardt algorithm.

The estimated kinetic constants: $k_1(T)$, $k_1(T_{ref})$, $k_2(T)$, $k_2(T_{ref})$, and a modified Arrhenius equation was expressed as follows:

$$k_1(T) = k_1(T_{ref}) * e^{\left[\frac{-E_{a1}}{R}\left(\frac{1}{T}-\frac{1}{T_{ref}}\right)\right]} \qquad \text{Equation 6}$$

$$k_2(T) = k_2(T_{ref}) * e^{\left[\frac{-E_{a1}}{R}\left(\frac{1}{T}-\frac{1}{T_{ref}}\right)\right]} \qquad \text{Equation 7}$$

From Table 4, one can notice that the credible interval for k1 is quite large, that could be explained by the fact that we do not measure the intermediate concentration.

Table 4. Estimated kinetic constants and statistical data

Parameters estimated at 15 ° C	Values	Credible interval	Credible interval in %
k1 (Tref :15°C) (L/mol/s)	0.14	+/- 0.14	97.50
Ea1 (J/mol)	0	-	-
kp (Tref :15°C) (L/mol/s)	0.08	+/- 0.01	9.10
Eap (J/mol)	48700.00	+/- 7760.0	15.90

From the preliminary modelling, it seems that the rate constant k_1 was temperature independent, for that reason we put Ea_1=0 J/mol.

The credible intervals for the other kinetic constants are narrow, meaning that the parameters are well identified.

The correlation matrix (Table 5) shows that the correlations are negligible in this case. According to Toch et al.,[46] two parameters are correlated if their binary correlation coefficient is higher than 0.95.

Table 5. Parameter correlation matrix

Parameters	k1 (L/mol/s)	kp (L/mol/s)	Eap (J/mol)
k1 (L/mol/s)	1.00	0.00	0.0
kp (L/mol/s)	-0.84	1.00	0.0
Eap (J/mol)	-0.49	0.49	1.0

Globally, Figures 5 and 6 show that the model can fit the experimental concentration of myrcene.

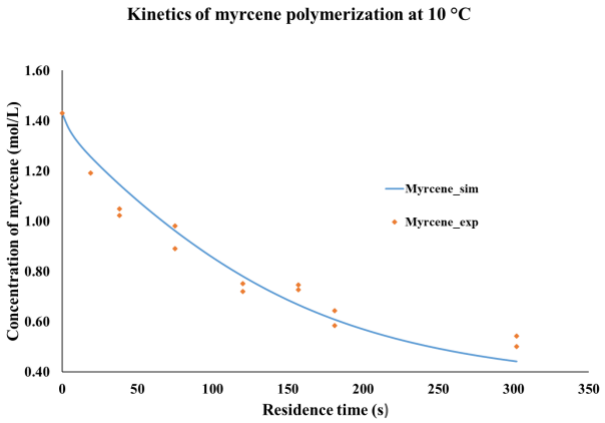

Fig. 5. Simulation vs experimental trend of concentration vs residence time at 10 ° C.

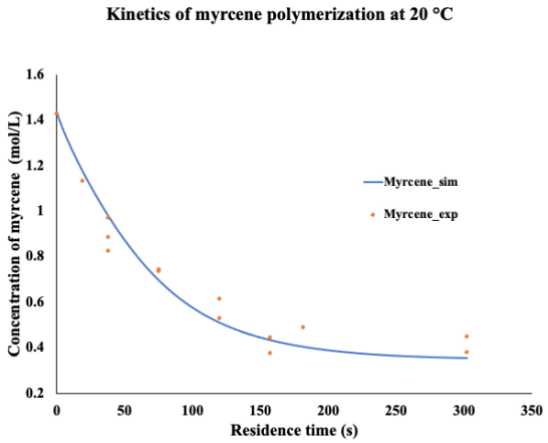

Fig. 6. Simulation vs experimental trend of concentration vs residence time at 20 ° C.

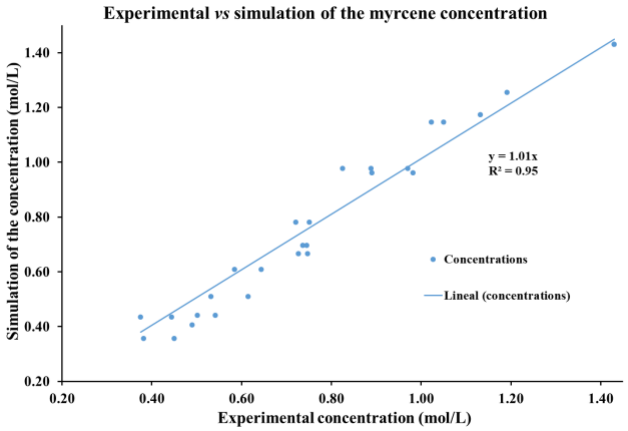

Fig. 7. Experimental concentration vs simulation concentration of myrcene (10 and 20 ° C).

Figure 7 (parity plot) shows that the model can predict the experimental concentrations.

End-functionalization of PMYR with CO_2 in a flow system

Feedstock-derived functional oligomers are attractive as molecular building blocks in replacing oil-based moieties. Among polyterpene derivatives amine ω-terminated β-myrcene polymers have been synthesized as well as hydroxytelechelic PMYR, these last being used as toughening agents.[47–49] To our knowledge acid end-groups have never been introduced on PMYR yet.[43,50–52]

As stated in the introduction, continuous flow systems exhibit higher mixing between chemical reagents, with major improvements in gas/liquid mass transfer. In this line, Yoshida and Jamison independently reported that the challenging trapping of CO_2, which often suffers from unselective consecutive competitive additions (carboxylic acid → ketone → tertiary alcohol) could be performed in a selective fashion in flow reactors.[53,54] Thus, a flow reactor system fed with an organometallic reagent (R-Li or R-MgX) in a first inlet, and a CO_2 tank connected to a mass flow controller in a second inlet provided the selective mono-addition product R-CO_2H without over-addition products, even without cryogenic conditions. Conversely, consecutive competitive over-addition occurred in batch reactors.[53,54] Based on these reports, we envisioned that the concatenated polymerization/CO_2H functionalization in flow synthesis of ketones would be a mean to overcome all the drawbacks associated with the analogous batch synthesis: 1) as shown above the Mn of PMYR can be finely tuned, 2) the higher interfacial contact between gas and liquid phases should enhance the selectivity of carboxylation. Moreover, it is possible to use stoichiometric amounts of CO_2 in flow, whereas it is generally much challenging under batch conditions. Thus, CO_2 was introduced in the previous flow set up implemented for the controlled anionic polymerization of myrcene was connected a third inlet connected to the CO_2 tank and controlled by mean of a mass flow controller (constant flow rate of 1.36 mL/min under 1 bar). The outlet was collected in an aqueous acidic solution (Figure 8).

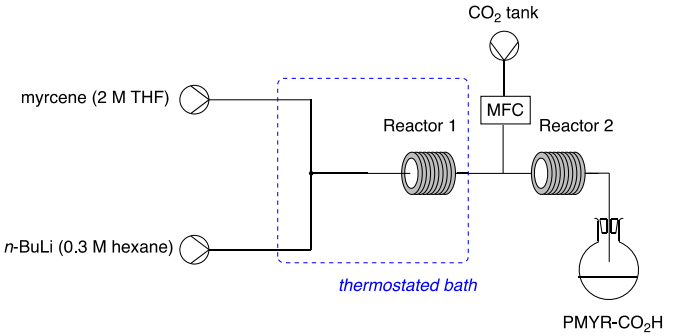

Fig. 8. Telescoped anionic polymerization of myrcene/functionalization with CO_2 in a flow system (MFC = mass flow controller).

Thus, after polymerization of myrcene in a stainless steel flow microreactor (ID = 0.75 mm, L = 3 m) as described above [Q(myrcene) = 0.25 mL/min, Q(*n*-BuLi) = 0.1 mL/min, t^R = 227 s] and CO_2 was delivered in a further inlet (Reactor 2: ID = 0.75 mm, L = 30 cm). Delightfully, this telescoped process afforded the target PMYR terminated by a useful CO_2H functional moiety PMYRCO_2H (Table 6, entries 3-5). Increasing the mass flow rate -and therefore increasing the number of equivalents of CO_2- allowed to reach a functionalization degree FD = 95% with 3 equiv. of gas with regard to *n*-BuLi.

Table 6. Experiments for the end-functionalization of PMYR with CO_2 at 10 °C.[a]

Entry	Conditions	*t* (s)[b]	Mass flow rate (mg/min)	Molar flow rate (mmol/min)	Molar ratio *n*-BuLi/CO_2	Mn (g/mol)		Đ	Product	FD (%)[c]
						^{1}H NMR	GPC			
1	batch	60	–	–	bubbled gas	1750	950	2.50	ketone	–
2	batch	120	–	–	bubbled gas	1800	1350	2.17	ketone	–
3	flow	7.6	1.32	0.03	1:1	1000	1200	1.58	acid	30
4	flow	4.6	2.64	0.06	1:2	1050	850	1.69	acid	64
5	flow	3.6	3.96	0.09	1:3	1415	1100	1.19	acid	95

[a] According to set-up described in Fig. 7. [b] Entries 1,2: bubbling time of CO_2 in the batch reactor; Entries 3-5: residence time in reactor 2 (t^{R2}). [c] Functionalization degree (FD) calculated by ^{1}H NMR by comparing the relative intensity of C*H*(CO_2H) (δ = 3.05 ppm) with the CH_3 group of butyl chain initiator of PMYR (δ = 0.86 ppm).

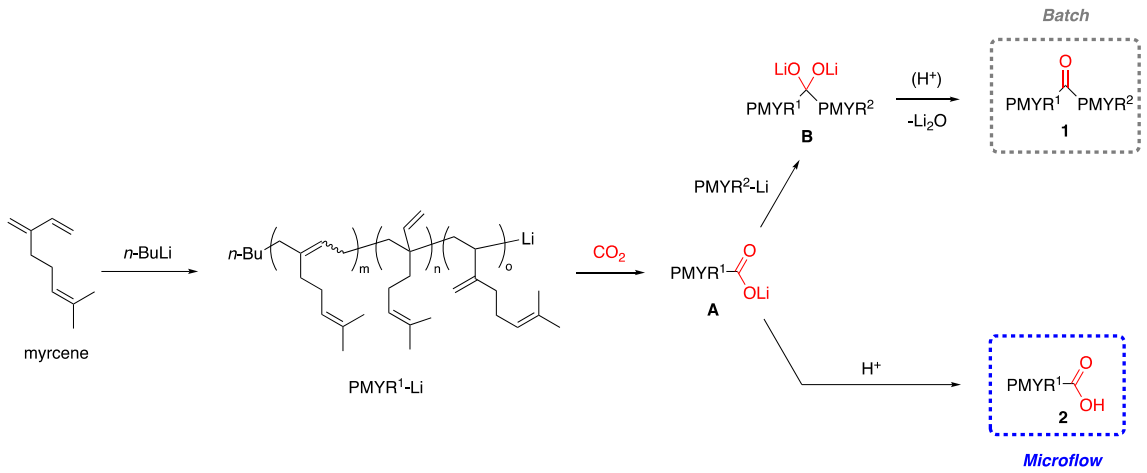

Fig. 9. End-functionalization of PMYR: reactivity according to batch or flow conditions.

It is worth to note that a parallel experiment was conducted under batch conditions (Table 6, entries 1 and 2) which afforded a different result: a ketone connected to two PMYR moieties was obtained as major product as attested by ^{13}C NMR in which a signal at δ = 207.19 ppm, typical of a -C(=O)- moiety appeared (in contrast to $\delta(CO_2)$ = 178.48 and 177.89 ppm detected in the flow experiment. This difference of reactivity (confirming thus the previous observations by Yoshida and Jamison with small organometallics) is depicted in Fig. 9, along with the corresponding reaction paths. Thus, in any reactor, PMYR-Li adds onto CO_2 to afford the intermediate **A**. Due to lower liquid/gas mass transfer in the batch reactor, there is, in this case, coexistence between PMYR-Li and **A** that can undergo a second addition to yield **B**. This latter, upon elimination of Li_2O, provides the ketone $(PMYR)_2C=O$ **1**. Beside mixing issues, a plausible explanation for this divergence of reactivity lies on a major dichotomy between batch and flow conditions: the composition of the reaction medium according to space and time. In a batch reactor, the chemical composition of the reaction medium evolves with time as the conversion of reagents/substrates to products increases. In contrast, under flow conditions, the conversion increases along the reactor: thus, any point of the flow reactor corresponds to a specific state of the progress of the reaction, with -ideally- a completion at the outlet of the reactor. In our case, this major feature avoids reactions between PMR-Li and the primary product **A**, and thus undesired competitive products, with high benefits for chemical selectivity toward $PMYR\text{-}CO_2H$ **2**.[55]

Conclusions

In conclusion, we have shown that the anionic polymerization of myrcene can be finely controlled under microfluidic conditions to yield custom polymyrcene (PMYR) oligomers. The common issues associated to mixing and temperature control, directly related to the amount of starting material used, are circumvented under these flow conditions. Moreover, a kinetic model has been developed that can perfectly predict the outcome of the polymerization. In addition, thanks to the microfluidic reactor, we have been able to trap CO_2, at the end of the polymerization, in a fully selective fashion to avoid the consecutive competitive reactions and introduce a useful carboxyl function. This work opens the door to a new sustainable process to obtain controlled and functionalized oligomers.

Conflicts of interest

There are no conflicts to declare.

Acknowledgements

The authors thank INSA Rouen Normandy, University of Rouen Normandy, the Centre National de la Recherche Scientifique (CNRS), Labex SynOrg (ANR-11-LABX-0029), Carnot Institute I2C, the graduate school for research XL-Chem (ANR-18-EURE-0020 XL CHEM) and Region Normandie for their support. Catherine Legrand and Denis Danvy (laboratory COBRA) are thanked for the SEC and IR analyses. K.P. is grateful to the Ministerio de Educación Superior, Ciencia y Tecnología of the Dominican Republic for the fellowship (CALIOPE Program).

Notes and references

1 P. A. Wilbon, F. Chu and C. Tang, *Macromol. Rapid Commun.*, 2013, **34**, 8–37.
2 P. Sahu, A. K. Bhowmick and G. Kali, *Processes*, 2020, **8**, 553.
3 N. Hadjichristidis, Y. Gnanou, K. Matyjaszewski and M. Muthukumar, Eds., *Macromolecular Engineering: From Precise Synthesis to Macroscopic Materials and Applications*, Wiley, 1st edn., 2022.
4 F. D. Monica and A. W. Kleij, *Polym. Chem.*, 2020, **11**, 5109–5127.
5 F. L. Hatton, *Polym. Chem.*, 2020, **11**, 220–229.
6 N. Bauer, J. Brunke and G. Kali, *ACS Sustain. Chem. Eng.*, 2017, **5**, 10084–10092.

7 A. Métafiot, L. Gagnon, S. Pruvost, P. Hubert, J.-F. Gérard, B. Defoort and M. Marić, *RSC Adv.*, 2019, **9**, 3377–3395.
8 P. Sahu, A. K. Bhowmick and G. Kali, *Processes*, 2020, **8**, 553.
9 S. Loughmari, A. Hafid, A. Bouazza, A. El Bouadili, P. Zinck and M. Visseaux, *J. Polym. Sci. Part A Polym. Chem.*, 2012, **50**, 2898–2905.
10 D. H. Lamparelli, M. M. Kleybolte, M. Winnacker and C. Capacchione, *Polymers*, 2021, **13**, 838.
11 P. Sahu, A. K. Bhowmick and G. Kali, *Processes*, 2020, **8**, 553.
12 J. Yoshida, H. Kim and A. Nagaki, *J. Flow Chem.*, 2017, **7**, 60–64.
13 T. Wirth, *Angew. Chem. Int. Ed.*, 2017, **56**, 682–684.
14 M. B. Plutschack, B. Pieber, K. Gilmore and P. H. Seeberger, *Chem. Rev.*, 2017, **117**, 11796–11893.
15 M. Movsisyan, E. I. P. Delbeke, J. K. E. T. Berton, C. Battilocchio, S. V. Ley and C. V. Stevens, *Chem. Soc. Rev.*, 2016, **45**, 4892–4928.
16 D. Dallinger, B. Gutmann and C. O. Kappe, *Acc. Chem. Res.*, 2020, **53**, 1330–1341.
17 B. Picard, B. Gouilleux, T. Lebleu, J. Maddaluno, I. Chataigner, M. Penhoat, F.-X. Felpin, P. Giraudeau and J. Legros, *Angew. Chem. Int. Ed.*, 2017, **56**, 7568–7572.
18 N. Emmanuel, P. Bianchi, J. Legros and J.-C. M. Monbaliu, *Green Chem.*, 2020, **22**, 4105–4115.
19 A. Delaune, S. Mansour, B. Picard, P. Carrasqueira, I. Chataigner, L. Jean, P.-Y. Renard, J.-C. M. Monbaliu and J. Legros, *Green Chem.*, 2021, **23**, 2925–2930.
20 S. Mansour, A. Delaune, M. Manneveau, B. Picard, A. Claudel, C. Vallières, L. Sigot, P.-Y. Renard and J. Legros, *Green Chem.*, 2021, **23**, 7522–7527.
21 P. Musci, T. von Keutz, F. Belaj, L. Degennaro, D. Cantillo, C. O. Kappe and R. Luisi, *Angew. Chem. Int. Ed.*, 2021, **60**, 6395–6399.
22 P. Musci, M. Colella, A. Sivo, G. Romanazzi, R. Luisi and L. Degennaro, *Org. Lett.*, 2020, **22**, 3623–3627.
23 M. Colella, A. Tota, Y. Takahashi, R. Higuma, S. Ishikawa, L. Degennaro, R. Luisi and A. Nagaki, *Angew. Chem. Int. Ed.*, 2020, **59**, 10924–10928.
24 B. Picard, K. Pérez, T. Lebleu, D. Vuluga, F. Burel, D. C. Harrowven, I. Chataigner, J. Maddaluno and J. Legros, *J. Flow Chem.*, 2020, **10**, 139–143.
25 K. Pérez, B. Picard, D. Vuluga, F. Burel, R. Hreiz, L. Falk, J.-M. Commenge, A. Nagaki, J. Yoshida, I. Chataigner, J. Maddaluno and J. Legros, *Org. Process Res. Dev.*, 2020, **24**, 787–791.
26 H. Kim, K.-I. Min, K. Inoue, D. J. Im, D.-P. Kim and J. Yoshida, *Science*, 2016, **352**, 691–694.
27 H. Kim, A. Nagaki and J. Yoshida, *Nat. Commun.*, 2011, **2**, 264.
28 H. Usutani, Y. Tomida, A. Nagaki, H. Okamoto, T. Nokami and J. Yoshida, *J. Am. Chem. Soc.*, 2007, **129**, 3046–3047.
29 T. Brégent, I. V. Ivanova, T. Poisson, P. Jubault and J. Legros, *Chem. – Eur. J.*, , DOI:10.1002/chem.202202286.
30 A. Nagaki, Y. Tomida and J. Yoshida, *Macromolecules*, 2008, **41**, 6322–6330.
31 A. Nagaki, Y. Tomida, A. Miyazaki and J. Yoshida, *Macromolecules*, 2009, **42**, 4384–4387.
32 A. Nagaki, A. Miyazaki and J. Yoshida, *Macromolecules*, 2010, **43**, 8424–8429.
33 C. Tonhauser, D. Wilms, F. Wurm, E. B. Nicoletti, M. Maskos, H. Löwe and H. Frey, *Macromolecules*, 2010, **43**, 5582–5588.
34 Y. Endo, M. Furusawa, T. Shimazaki, Y. Takahashi, Y. Nakahara and A. Nagaki, *Org. Process Res. Dev.*, 2019, **23**, 635–640.
35 A. Nagaki, H. Yamashita, Y. Tsuchihashi, K. Hirose, M. Takumi and J. Yoshida, *Chem. – Eur. J.*, 2019, **25**, 13719–13727.
36 J. M. Bolton, M. A. Hillmyer and T. R. Hoye, *ACS Macro Lett.*, 2014, **3**, 717–720.
37 P. Stanetty and M. D. Mihovilovic, *J. Org. Chem.*, 1997, **62**, 1514–1515.
38 J. Clayden, *Nat. Chem.*, 2010, **2**, 523–524.
39 J. Clayden and S. A. Yasin, *New J. Chem.*, 2002, **26**, 191–192.
40 A. Ávila-Ortega, M. Aguilar-Vega, M. I. Loría Bastarrachea, C. Carrera-Figueiras and M. Campos-Covarrubias, *J. Polym. Res.*, 2015, **22**, 226.
41 J. M. Bolton, M. A. Hillmyer and T. R. Hoye, *ACS Macro Lett.*, 2014, **3**, 717–720.
42 J. Zhang, C. Aydogan, G. Patias, T. Smith, L. Al-Shok, H. Liu, A. M. Eissa and D. M. Haddleton, *ACS Sustain. Chem. Eng.*, 2022, **10**, 9654–9664.
43 J. González-Villa, E. Saldívar-Guerra, R. E. D. de León-Gómez, H. R. López González and J. R. Infante-Martínez, *J. Polym. Sci. Part Polym. Chem.*, 2019, **57**, 2157–2165.
44 J. L. Zheng, J. Wärnå, T. Salmi, F. Burel, B. Taouk and S. Leveneur, *AIChE J.*, 2016, **62**, 726–741.
45 S. Leveneur, M. Pinchard, A. Rimbault, M. Safdari Shadloo and T. Meyer, *Thermochim. Acta*, 2018, **666**, 10–17.
46 K. Toch, J. W. Thybaut and G. B. Marin, *AIChE J.*, 2015, **61**, 880–892.
47 S. Georges, O. H. Hashmi, M. Bria, P. Zinck, Y. Champouret and M. Visseaux, *Macromolecules*, 2019, **52**, 1210–1219.
48 A. Ávila-Ortega, M. Aguilar-Vega, M. I. Loría Bastarrachea, C. Carrera-Figueiras and M. Campos-Covarrubias, *J. Polym. Res.*, 2015, **22**, 226.
49 C. Zhou, Z. Wei, X. Lei and Y. Li, *RSC Adv.*, 2016, **6**, 63508–63514.
50 C. Wahlen and H. Frey, *Macromolecules*, 2021, **54**, 7323–7336.
51 A. Métafiot, Y. Kanawati, J.-F. Gérard, B. Defoort and M. Marić, *Macromolecules*, 2017, **50**, 3101–3120.
52 E. Grune, J. Bareuther, J. Blankenburg, M. Appold, L. Shaw, A. H. E. Müller, G. Floudas, L. R. Hutchings, M. Gallei and H. Frey, *Polym. Chem.*, 2019, **10**, 1213–1220.
53 J. Wu, X. Yang, Z. He, X. Mao, T. A. Hatton and T. F. Jamison, *Angew. Chem. Int. Ed.*, 2014, **53**, 8416–8420.
54 A. Nagaki, Y. Takahashi and J. Yoshida, *Chem. – Eur. J.*, 2014, **20**, 7931–7934.
55 J.-C. M. Monbaliu and J. Legros, *Lab. Chip*, DOI:10.1039/D2LC00796G.